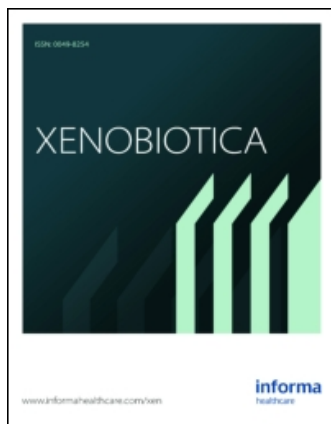


This article was downloaded by: [University of Exeter]

On: 14 August 2015, At: 17:14

Publisher: Taylor & Francis

Informa Ltd Registered in England and Wales Registered Number: 1072954 Registered office: 5 Howick Place, London, SW1P 1WG



Xenobiotica: the fate of foreign compounds in biological systems

Publication details, including instructions for authors and subscription information:

<http://www.tandfonline.com/loi/ixen20>

Structural elucidation of in vitro metabolites of bavachinin in rat liver microsomes by LC-ESI-MSⁿ and chemical synthesis

Fan Xie^a, Guoxin Du^a, Shunan Ma^a, Yiming Li^a, Rui Wang^a & Fujiang Guo^a

^a School of Pharmacy, Shanghai University of Traditional Chinese Medicine, Shanghai, P. R. China

Published online: 14 Aug 2015.



[Click for updates](#)

To cite this article: Fan Xie, Guoxin Du, Shunan Ma, Yiming Li, Rui Wang & Fujiang Guo (2015): Structural elucidation of in vitro metabolites of bavachinin in rat liver microsomes by LC-ESI-MSⁿ and chemical synthesis, *Xenobiotica: the fate of foreign compounds in biological systems*

To link to this article: <http://dx.doi.org/10.3109/00498254.2015.1074763>

PLEASE SCROLL DOWN FOR ARTICLE

Taylor & Francis makes every effort to ensure the accuracy of all the information (the "Content") contained in the publications on our platform. However, Taylor & Francis, our agents, and our licensors make no representations or warranties whatsoever as to the accuracy, completeness, or suitability for any purpose of the Content. Any opinions and views expressed in this publication are the opinions and views of the authors, and are not the views of or endorsed by Taylor & Francis. The accuracy of the Content should not be relied upon and should be independently verified with primary sources of information. Taylor and Francis shall not be liable for any losses, actions, claims, proceedings, demands, costs, expenses, damages, and other liabilities whatsoever or howsoever caused arising directly or indirectly in connection with, in relation to or arising out of the use of the Content.

This article may be used for research, teaching, and private study purposes. Any substantial or systematic reproduction, redistribution, reselling, loan, sub-licensing, systematic supply, or distribution in any form to anyone is expressly forbidden. Terms & Conditions of access and use can be found at <http://www.tandfonline.com/page/terms-and-conditions>

RESEARCH ARTICLE

Structural elucidation of *in vitro* metabolites of bavachinin in rat liver microsomes by LC-ESI-MSⁿ and chemical synthesis

Fan Xie, Guoxin Du, Shunan Ma, Yiming Li, Rui Wang, and Fujiang Guo

School of Pharmacy, Shanghai University of Traditional Chinese Medicine, Shanghai, P. R. China

Abstract

1. Bavachinin isolated from *Psoralea corylifolia* has various activities, such as antimicrobial, antiallergic, antitumor and so on. Our previous study showed that natural bavachinin exhibits peroxisome proliferator-activated receptor γ -agonist activity.
2. *In vitro* studies on bavachinin metabolism were conducted using rat liver microsomes incubated at 37 °C for 60 min.
3. Structures of eight metabolites of the incubation mixtures were cautiously characterized using electrospray tandem mass spectra and three synthetic compounds. The results indicated that eight metabolites of bavachinin were biotransformed mainly through oxidation.
4. The metabolic pathways of bavachinin were elucidated *in vitro*. These results contribute to the understanding of bavachinin's *in vivo* metabolism.

Keywords

Bavachinin, chemical synthesis, *in vitro* metabolism, mass spectrometry, rat liver microsomes

History

Received 17 June 2015
Revised 15 July 2015
Accepted 16 July 2015
Published online 10 August 2015

Introduction

Dry and ripe seeds of leguminous plant *Psoralea corylifolia* L. (bu-gu-zhi in Chinese) have been widely used for treating asthma, diarrhea, waist and knee psychoralgia (Luo et al., 2014), osteoporosis (Huang et al., 2014; Li et al., 2014), kidney insufficiency, enuresis, vitiligo and alopecia areata (Pharmacopeia Committee of P.R. China, 2010). Most of its chemical constituents, including flavonoids, furanocoumarins and monoterpene phenols, have been isolated, a few of which exhibit antioxidant (Guo et al., 2005), antimicrobial and hepatoprotective activities (Chopra et al., 2013); DNA polymerase and topoisomerase II inhibition (Sun et al., 1998); and antidermatophytic (Lau et al., 2014), antiallergic (Matsuda et al., 2007) and antitumor (Chen et al., 2010) activities.

Bavachinin (Figure 1), isolated from *P. corylifolia* (Chen et al., 2012), is a prenylated flavonoid. Bavachinin exhibits antiallergic, anti-inflammatory (Chen et al., 2013, 2014), antiangiogenic, antitumor (Nepal et al., 2012) and antioxidant activities (Xiao et al., 2010), and inhibits severe acute respiratory syndrome coronavirus papain-like protease (Kim et al., 2014). In our study (WO2014/169800), natural bavachinin exhibited peroxisome proliferator-activated receptor γ (PPAR- γ) agonist activity. PPARs are members of the

nuclear hormone receptors' superfamily and are essential in the regulation of cellular differentiation, development, metabolism and tumorigenesis of higher organisms (Singh et al., 2011). PPAR- γ is a key regulator of insulin sensitization and glucose metabolism (Chigurupati et al., 2015), and PPAR- γ activation is extremely effective in improving glycemic management; however, little is known about the metabolism of bavachinin.

In vitro metabolic studies are gaining increasing attention for several reasons, including their speediness, simplicity, convenience and low cost. Moreover, *in vitro* metabolism studies can eliminate the disturbance of factors *in vivo* to observe the selective metabolism of metabolic enzyme on substrate, which will get more reliable theory basis for *in vivo* metabolism. Methods used to study the *in vitro* metabolism studies of flavonoids include the Caco-2 cell model, gastrointestinal contents hatching, the enterohepatic microsomal method, and the genetic recombination metabolic enzyme method (Aura et al., 2005; Boersma et al., 2002; Chen et al., 2005; Si et al., 2009). Except these, liver microsomes play an important role in researching the metabolism of flavonoids, because the liver is the crucial metabolism site (Wang & Ho, 2009). Several studies on the metabolism of flavonoids in liver microsomes have been reported (Lee et al., 2007; Nikolic et al., 2005; Quintieri et al., 2008).

The aim of this study is to identify the metabolites of bavachinin in rat liver microsomes and to speculate the metabolic pathways of bavachinin by mass spectrometry combined with liquid chromatography and chemical synthesis.

Address for correspondence: Prof. Fujiang Guo and Prof. Rui Wang, School of Pharmacy, Shanghai University of Traditional Chinese Medicine, 1200 Cailun Road, Shanghai, 201203, P. R. China. Tel: + 86 21 51322181. Fax: + 86 21 51322193. E-mail: gfgj@shutcm.edu.cn (F. Guo); ellewang@163.com (R. Wang).

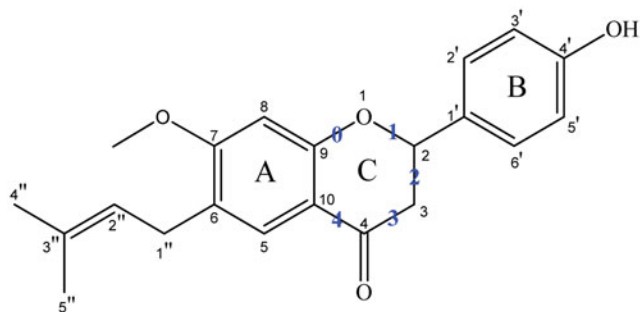


Figure 1. Molecular structure of bavachinin.

Materials and methods

Chemicals

Bavachinin was isolated from *P. corylifolia* L as previously described (Yin et al., 2004); its purity was determined to be >98% by using a high-performance liquid chromatography (HPLC) analysis (Hyper ODS2 C₁₈ column; 4.6 mm × 250 mm, 5 μm). Separation was performed under the following conditions: flow rate, 1.0 mL/min; solvent A, 0.3% phosphoric acid in water; solvent B, CH₃CN; 0–15 min, 50–95% B; 15–20 min, 95–95% B; 20–25 min, 95–50% B (v/v). HPLC-grade solvents were purchased from Fisher Scientific Co. (Fair Lawn, NJ). All other chemicals were purchased from Sinopharm Chemical Reagent Co. (Shanghai, China).

Synthesis of 4'-hydroxy-7-methoxy-6-(3-methyl-2-butenyl)-flavone (S1b)

Iodine (94 mg, 0.74 mM) was added to a solution of bavachinin (S1a) (250 mg, 0.74 mM) in DMSO (10 mL). The mixture was heated to 90 °C and stirred for 3 h. The reaction mixture was monitored through thin layer chromatography (TLC). After cooling, the reaction mixture was diluted with water and the iodine was removed by washing with saturated sodium thiosulfate solution (20 mL). The product was extracted using ethyl acetate (2 × 20 mL). The organic layers were combined, washed using saturated sodium chloride solution (NaCl, 10 mL), dried over sodium sulfate (Na₂SO₄), filtrated and evaporated in vacuum. The crude material was purified by silica gel column chromatography with petroleum ether/ethyl acetate to yield a pale yellow powder, S1b (122 mg, 49.09%) (Scheme 1). ¹H NMR (400 MHz, DMSO-d₆) δ 10.28 (s, 1H), 7.95 (d, *J* = 8.8 Hz, 2H), 7.70 (s, 1H), 7.29 (s, 1H), 6.93 (d, *J* = 8.8 Hz, 2H), 6.78 (s, 1H), 5.30 (t, *J* = 7.5 Hz, 1H), 3.96 (s, 3H), 3.32 (d, *J* = 7.4 Hz, 2H), 1.74 (s, 3H), 1.68 (s, 3H). ¹³C NMR (100 MHz, DMSO-d₆) δ 176.2, 162.4, 161.5, 160.7, 156.0, 132.7, 128.0, 128.0, 123.9, 121.7, 121.4, 116.4, 115.8, 104.6, 99.3, 56.3, 27.6, 25.5, 17.6. LR-ESI-MS *m/z*: 337.3 [M + H]⁺; 335.1 [M – H]⁺. HR-ESI-MS measured 337.1441 ([M + H]⁺, calcd 337.1440 for C₂₁H₂₁O₄).

Synthesis of 3',4'-dihydroxy-7-methoxy-6-(3-methyl-2-butenyl)-flavanone (S2f)

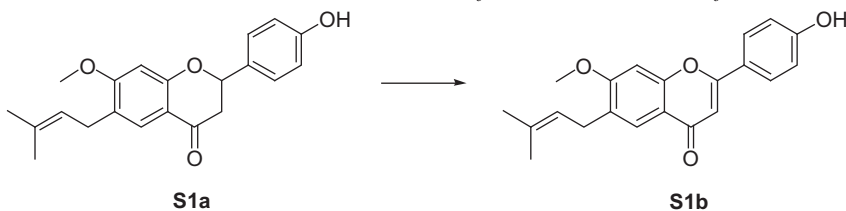
Chloromethyl methyl ether (714 mg, 8.87 mM) was added slowly to a stirred solution of S2a (500 mg, 3.62 mM) and anhydrous K₂CO₃ (2000 mg, 14.47 mM) in dry acetone

(20 mL) at room temperature and stirred for 2 h (Scheme 2). The reaction mixture was monitored using TLC. The reaction mixture was quenched using water (40 mL) and extracted using ethyl acetate (2 × 20 mL). The organic layers were combined, washed using a saturated NaCl solution (20 mL), dried over Na₂SO₄, filtrated and evaporated in vacuum. The residue was purified by silica gel column chromatography with petroleum ether/ethyl acetate to yield a colorless oil, S2b (646 mg, 78.88%). Potassium trimethylsilylanolate (1320 mg, 9.19 mM) was added to a stirred solution of S2c (652 mg, 2.78 mM) and S2b (630 mg, 2.78 mM) in ethanol (20 mL), and the mixture was refluxed in an inert atmosphere for 4 h. The reaction mixture was monitored using TLC. The reaction mixture was quenched using saturated aqueous NH₄Cl (20 mL) and extracted using ethyl acetate (2 × 20 mL). The organic layers were processed as previously described to yield S2d as bright yellow needles (460.3 mg, 37.38%). Potassium fluoride (230 mg, 3.96 mM) was added to a solution of S2d (460.3 mg, 1.04 mM) in methanol (10 mL). The mixture was refluxed with stirring for 8 h. The reaction mixture was monitored using TLC. The reaction mixture was quenched and extracted using water (10 mL) and ethyl acetate (2 × 10 mL), respectively. The organic layers were processed as previously described to yield S2e as a white solid (269.3 mg, 58.51%). Aqueous hydrochloric acid (3 N, 2.26 mL) was added to a solution of S2e (200 mg, 0.45 mM) in methanol (7 mL), and the mixture was refluxed for 10 min. After cooling and diluting with water (10 mL), the mixture was extracted using ethyl acetate (2 × 10 mL). The organic layers were processed as previously described to yield S2f as a pale yellow solid (96.5 mg, 60.24%). ¹H NMR δ (400 MHz, DMSO-d₆) 9.07 (s, 1H), 9.02 (s, 1H), 7.47 (s, 1H), 6.90 (s, 1H), 6.78–6.73 (m, 2H), 6.60 (s, 1H), 5.40 (dd, *J* = 12.7, 3.0 Hz, 1H), 5.23 (t, *J* = 7.5 Hz, 1H), 3.84 (s, 3H), 3.18 (d, *J* = 7.4 Hz, 2H), 3.06 (dd, *J* = 16.8, 12.7 Hz, 1H), 2.63 (dd, *J* = 16.8, 3.0 Hz, 1H), 1.71 (s, 3H), 1.65 (s, 3H). ¹³C NMR δ (100 MHz, DMSO-d₆) 190.4, 163.4, 161.9, 145.6, 145.2, 132.2, 129.8, 126.0, 123.4, 121.9, 117.9, 115.3, 114.3, 113.5, 99.3, 79.2, 56.1, 43.2, 27.3, 25.6, 17.6. LR-ESI-MS *m/z*: 355.1 [M + H]⁺. HR-ESI-MS measured 355.1535 ([M + H]⁺, calcd 355.1545 for C₂₁H₂₃O₅).

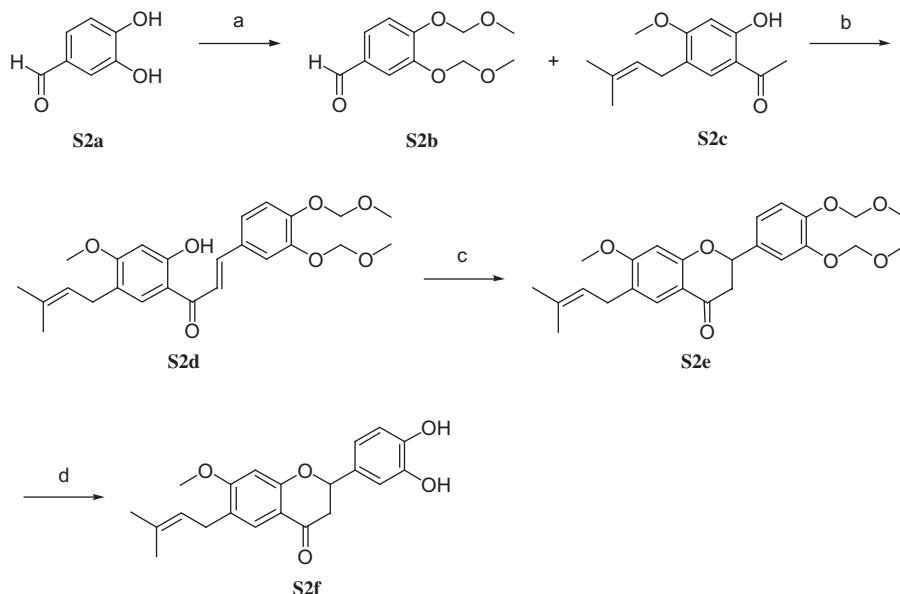
Preparation of (E)-4'-hydroxy-7-methoxy-6-(4-hydroxy-3-methyl-2-butenyl)-flavanone

The microorganism, *Cunninghamella elegans* AS 3.2028, was transferred in turn from slants to conical flasks of 500 mL containing 150 mL of potato media. The flasks were incubated at 25 °C with rotary shaking at 160 rpm. After 2 days, 15 mg of a biologically transformable substrate was dissolved in 1.5 mL acetone, added to each flask, and incubated with shaking for 5 days. The mixture was filtered, and extracted for three times with ethyl acetate (3 × 150 mL). After a sufficient quantity of the transformed product accumulated, it was isolated and purified by column chromatography or semipreparative HPLC (Scheme 3), to yield a light yellow amorphous powder, which was confirmed as C₂₁H₂₂O₅ by high-resolution electrospray ionization mass spectrometry (HR-ESI-MS) at *m/z* 377.1371 [M + Na]⁺. ¹H-NMR (600 MHz, CD₃OD): δ 7.60 (s, 1H, H-5), 7.34

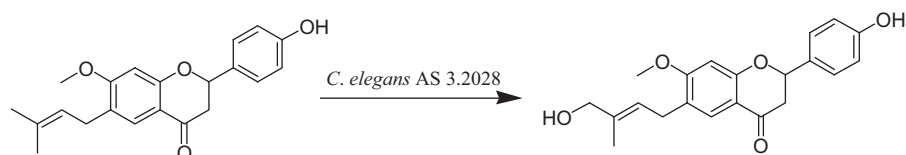
Scheme 1. Reagents and conditions: (a) I₂, DMSO, 90 °C, 3 h (49.09%).



Scheme 2. Reagents and conditions: (a) MOMCl, K₂CO₃, acetone, room temperature, 2 h; (b) (CH₃)₃SiO⁻K⁺, C₂H₅OH, reflux, 4 h; (c) KF, CH₃OH, reflux, 8 h; (d) HCl, CH₃OH, reflux, 10 min.



Scheme 3. Biotransformation of bavachinin by *C. elegans* AS 3.2028.



(d, $J = 8.5$ Hz, 2H, H-2',6'), 6.82 (d, $J = 8.5$ Hz, 2H, H-3', 5'), 6.55 (s, 1H, H-8), 5.55 (t, 1H, H-2''), 5.40 (dd, $J = 13.2, 2.9$ Hz, 1H, H-2), 3.97 (s, 2H, H-4''), 3.88 (s, 3H, H-12), 3.07 (dd, $J = 16.9, 13.2$ Hz, 1H, H-3 a), 2.71 (dd, $J = 16.9, 2.9$ Hz, 1H, H-3 b), 1.74 (s, 3H, H-5''). ¹³C-NMR (150 MHz, CD₃OD): δ 193.8 (C-4), 165.9 (C-7), 164.5 (C-9), 159.0 (C-4'), 137.4 (C-3''), 131.3 (C-1'), 129.0 (C-5), 127.8 (C-2', 6'), 125.3 (C-2''), 123.9 (C-6), 116.3 (C-10), 114.9 (C-3', 5') 100.0 (C-8), 81.3 (C-2), 68.8 (C-4''), 56.5 (C-12), 44.9 (C-3), 28.3 (C-1''), 13.7 (C-5'').

Rat liver microsomes

Rats were individually weighed and decollated to prepare liver microsomes. Livers were perfused using ice-cold saline followed by mincing and homogenizing with three volumes of 100 mM phosphate buffer (pH 7.4, containing 0.15 M KCl). The homogenates were centrifuged at 9000 *g* for 30 min at 4 °C. Subsequently, the supernatants were centrifuged at 105 000 *g* for 60 min at 4 °C to isolate liver microsomes, which were resuspended in 100 mM phosphate buffer (K₂HPO₄-KH₂PO₄, pH 7.4) and stored at -80 °C until further use (Bi et al., 2015).

Microsomal incubation procedure

A mixture (0.1 mL) containing 0.5 mg/mL of rat liver microsomes, 200 μM bavachinin, 10 mM MgCl₂ and 2 mM NADPH in 50 mM Tris-HCl buffer (pH 7.4) was incubated at 37 °C in a temperature-controlled water bath for 60 min. The mixture was preincubated for 5 min at 37 °C prior to NADPH addition. The reaction was stopped using 0.1 mL cold methanol to precipitate the proteins. The reaction vial was stored at -20 °C for 30 min. Subsequently, the samples were centrifuged and the supernatants were analyzed by LC-MS. Control samples were incubated without substrate or without NADPH (Nikolic et al., 2004).

Apparatus and analytical conditions

Analyses were performed using a Shimadzu UFLC-XR HPLC system (Shimadzu Scientific Inc., Kyoto, Japan) coupled with a LCQ ion trap mass spectrometer system (Thermo Fisher Scientific, Waltham, MA). An XSELECT HSS T3 column (2.1 mm × 150 mm, 3.5 μm) (Waters, Milford, MA) was used for the LC analysis. Metabolite separation was conducted under the following conditions: flow rate, 0.2 mL/min; solvent A, 0.05% HCOOH; solvent B, CH₃CN; 0–8 min, 40–74% B;

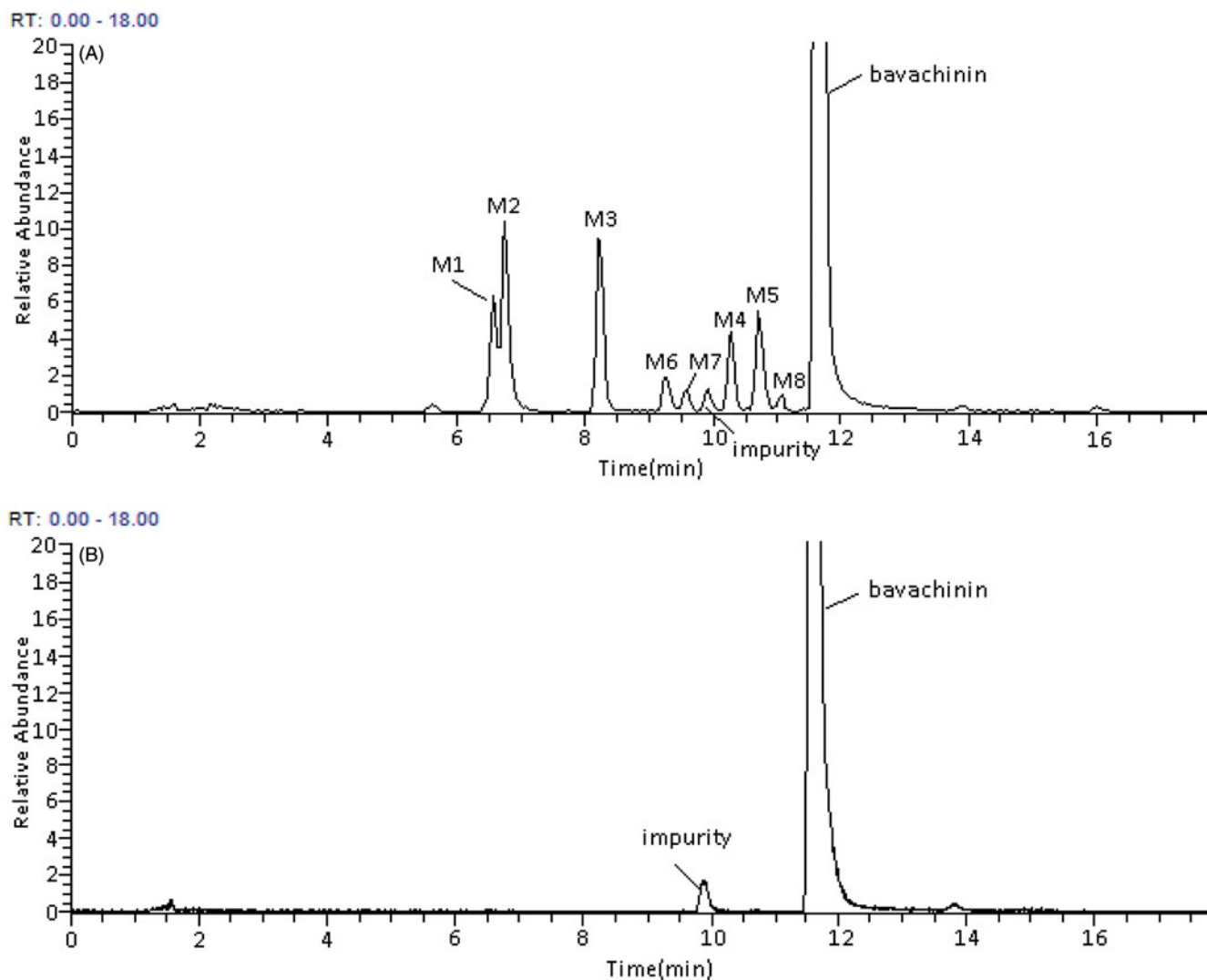


Figure 2. Computer-reconstructed, selected ion chromatogram for the positive ion electrospray LC-MS analysis of an incubation of bavachinin and pooled rat liver microsomes. (A) 60 min (B) 0 min. Selected ions were m/z 337, 339, 355.

8–13 min, 74–80% B; 13–18 min, 80–90% B (v/v). ESI was performed in the positive mode at a spray voltage of 4.5 kV; the capillary voltage and tube lens were set at -45 V and -125 V, respectively. The sheath gas flow rate was 40 (arbitrary units) and the aux gas flow rate was 10 (arbitrary units). The capillary temperature was set to 320°C . Normalized collision energy of 20–35% was applied to ions for the MS^n experiments.

Results and discussion

Metabolism of bavachinin in rat liver microsomes

The computer-reconstructed, selected ion chromatogram (m/z 337, 339, 355) for the positive ion electrospray LC-MS analysis of the incubation mixture of bavachinin, and pooled liver microsomes is shown in Figure 2(A). Compared with the control groups, eight peaks were eluted before bavachinin (t_R 11.7 min) in the LC-MS profile, including five major peaks (metabolite 1, t_R 6.6 min; metabolite 2, t_R 6.8 min; metabolite 3, t_R 8.2 min; metabolite 4, t_R 10.3 min; metabolite 5, t_R 10.7 min), three minor peaks (metabolite 6, t_R 9.3 min; metabolite 7, t_R 9.6 min; metabolite 8, t_R 11.1 min). These eight metabolites were absent from the incubation mixture at

0 min (Figure 2B) and increased with time. The MS^n experiments were subsequently employed to analyze the fragmentation pathways of bavachinin and the eight metabolites. Positive ESI MS^n spectra are presented in Figure 3.

Mass spectral fragmentation of bavachinin

A molecular ion peak $[\text{M} + \text{H}]^+$ at m/z 339 was seen in the positive ESI full-scan mass spectrum of bavachinin. In the MS^2 spectrum, the ion at m/z 321 was produced by the elimination of an H_2O molecule from the ion at m/z 339 (Ma et al., 1997), and two abundant fragment ions at m/z 283 and 271 were generated (Figure 3A). The ion at m/z 271 was produced by the elimination of the prenyl chain from the ion at m/z 339 (Xu et al., 2012), whereas the ion at m/z 283 was produced by the loss of isobutylene chain $[(\text{CH}_3)_2\text{C} = \text{CH}_2]$ from the ion at m/z 339 (Su et al., 2015), which exhibited a stable benzyl structure (Nikolic et al., 2004). The preceding two pathways can be used for the inference of metabolism occurring in the prenyl group. The product ions at m/z 283 and 271 fragmented into ions at m/z 189 and 177 by ring B elimination (Simons et al., 2009). According to a previous report (Fabre et al., 2001), bavachinin can also produce a

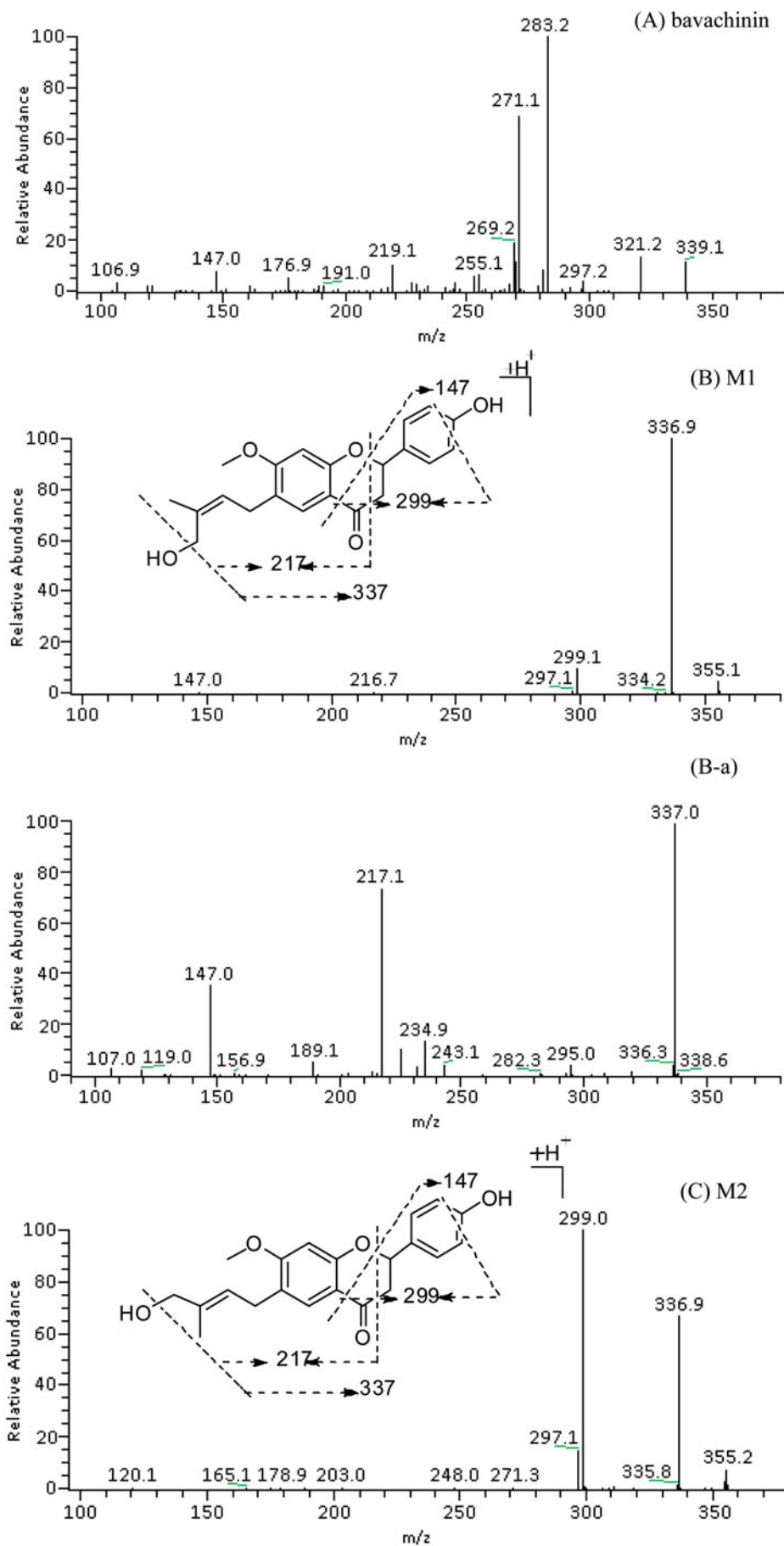


Figure 3. The MS² spectra of protonated bavachinin (A), M1 (B), M2 (C), M3 (D), M4 (E), M5 (F), M6 (G), M7 (H) and M8 (I) obtained by ion trap mass spectrometry. The MS³ spectra of the ions at *m/z* 337 of M1 (B-a) and M2 (C-a), *m/z* 283 of M3 (D-a) obtained through ion trap mass spectrometry.

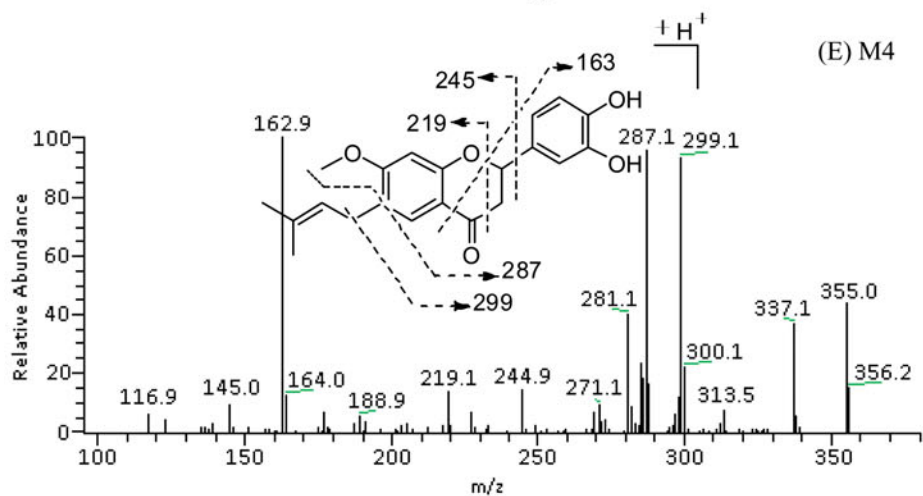
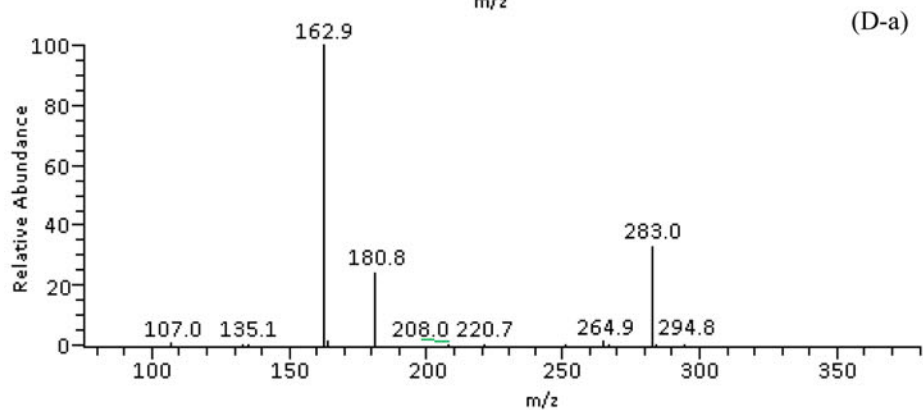
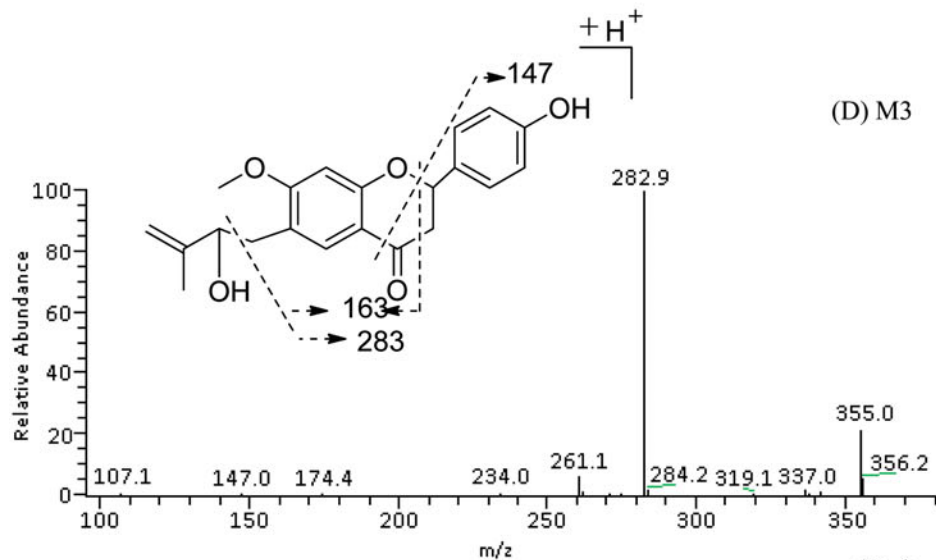
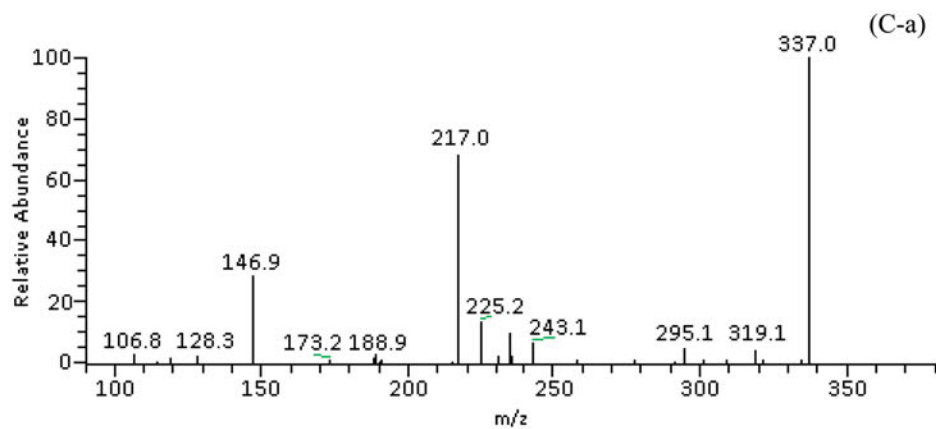


Figure 3. Continued.

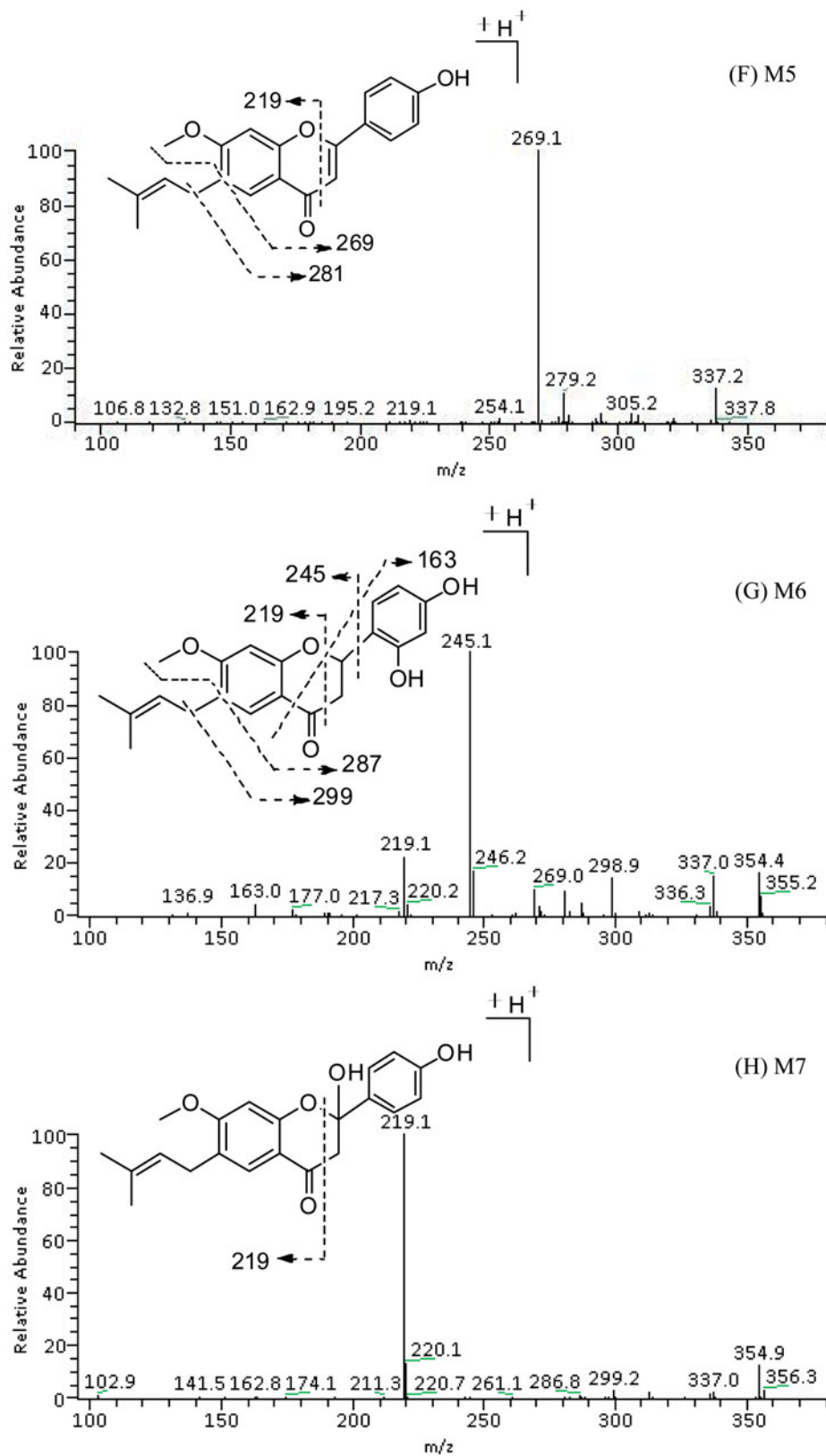


Figure 3. Continued.

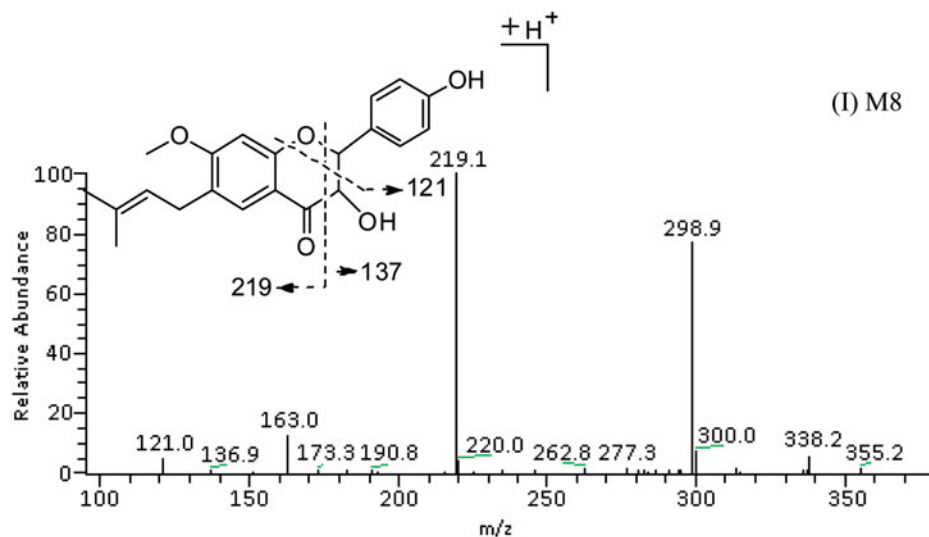


Figure 3. Continued.

typical fragment ion ($^{1,3}A^+$ ion) of flavonoids at m/z 219 by a retro-Diels-Alder (RDA) reaction on ring C. In addition, $^{1,4}B^+$ ion at m/z 147 was formed by a cleavage of bond 1,4 on ring C (Simons et al., 2009). The main fragmentation pathways are illustrated in Figure 4.

Identification of the metabolites of bavachinin

In the positive ESI full-scan mass spectrum, metabolites **M1-4** and **M6-8** produced the same protonated molecule $[M + H]^+$ at m/z 355, whereas metabolite **M5** produced an ion at m/z 337. The mass measurements of **M1-4** and **M6-8** corresponded to an elemental composition of $C_{21}H_{22}O_5$, suggesting that they were hydroxylated products of bavachinin. The molecular mass and retention time of **M5** indicate that it may be an oxidative product of bavachinin.

In the MS^2 spectrum of **M1** (Figure 3B), the ions at m/z 337 and 299 were the most abundant fragment ions of m/z 355. The ion at m/z 299 was formed by the keto group elimination of ring C and by the loss of the CO group of ring B (Zhang et al., 2014). The ion at m/z 337 may have formed by eliminating an H_2O molecule from **M1** (Ma et al., 1997). In addition, the ion at m/z 147 was formed, indicating that ring B was intact (Simons et al., 2009). Moreover, ion at m/z 217 was produced by the RDA reaction on ring C of the ion at m/z 337 (Fabre et al., 2001), suggesting that the prenyl chain was oxidized. **M1** and **M2** may be cis-trans isomers because of similar product ion mass spectra (Figure 3C). **M2** was identified as trans 4'-hydroxy-7-methoxy-6-(4-hydroxy-3-methyl-2-butenyl)-flavanone by comparing the retention time in the TIC and molecular weight with those of synthetic trans 4'-hydroxy-7-methoxy-6-(4-hydroxy-3-methyl-2-butenyl)-flavanone (Ma et al., 2015), whereas **M1** could be the geometric isomer of **M2**, cis 4'-hydroxy-7-methoxy-6-(4-hydroxy-3-methyl-2-butenyl)-flavanone.

The mass spectrum of **M3** revealed little information (Figure 3D). The loss of water molecule (m/z 337) from the ion at m/z 355 suggested the presence of a hydroxyl group near a double bond for the formation of a stable conjugated structure. The fragment ion at m/z 283 and the ion at m/z 284

corresponded to losses of 71–72 mass units, which might be containing four carbon atoms and one oxygen atom; the additional oxygen added to **M3** could not be located on the benzylic carbon (Nikolic et al., 2004). The ion at m/z 283 was fragmented through the RDA reaction on ring C to form the ion at m/z 163. In addition, $^{1,4}B^+$ ion at m/z 147 was also formed through the cleavage of bond 1,4 at ring C as bavachinin (Simons et al., 2009). These major fragmentation pathways indicate that the prenyl chain was oxidized. On the basis of several relevant studies (Nikolic et al., 2004, 2005), we speculate that C-2'' of the prenyl chain was oxidized, thus yielding a more stable structure.

Several fragmentation pathways of **M4** were similar to those of bavachinin. For example, based on the loss of H_2O , the ion of m/z 355 produced an ion of m/z 337 (Ma et al., 1997) (Figure 3E). The ions at m/z 299, 287 and 163 were the three most abundant fragment ions. The ion at m/z 299 was produced by the loss of isobutylene chain $[(CH_3)_2C=CH_2]$ from the ion at m/z 355 (Su et al., 2015), whereas the ion at m/z 287 was formed by the elimination of prenyl chain from the ion at m/z 355 (Xu et al., 2012). The ion at m/z 163 ($^{1,4}B^+$) was also formed by a cleavage of bond 1,4 at ring C as bavachinin (Simons et al., 2009). Finally, ring C underwent a RDA reaction to form the ion of m/z 219. The fragmentation pathways indicate that ring B may have been oxidized; the synthetic 3',4'-dihydroxy-7-methoxy-6-(3-methyl-2-butenyl)-flavanone further supported this observation. Many fragmentation pathways of **M4** and **M6** were similar (Figure 3G). Moreover, **M6** generated a main fragment ion at m/z 245 through a cleavage of the single bond between ring B and ring C, indicating that ring B was oxidized. Thus, **M6** was identified as 2',4'-dihydroxy-7-methoxy-6-(3-methyl-2-butenyl)-flavanone.

M5 produced a protonated molecule at m/z 337 during positive ion electrospray, and was considered to be an oxidative product of bavachinin. The ions at m/z 281 and 269 in the MS^2 spectrum (Figure 3F) corresponded to m/z 283 and 271 in the MS^2 spectrum of bavachinin. The ion at m/z 269 was formed through the elimination of the prenyl chain from the ion of m/z 337, whereas the ion at m/z 281 was produced

Figure 4. Main fragmentation pathways of bavachinin.

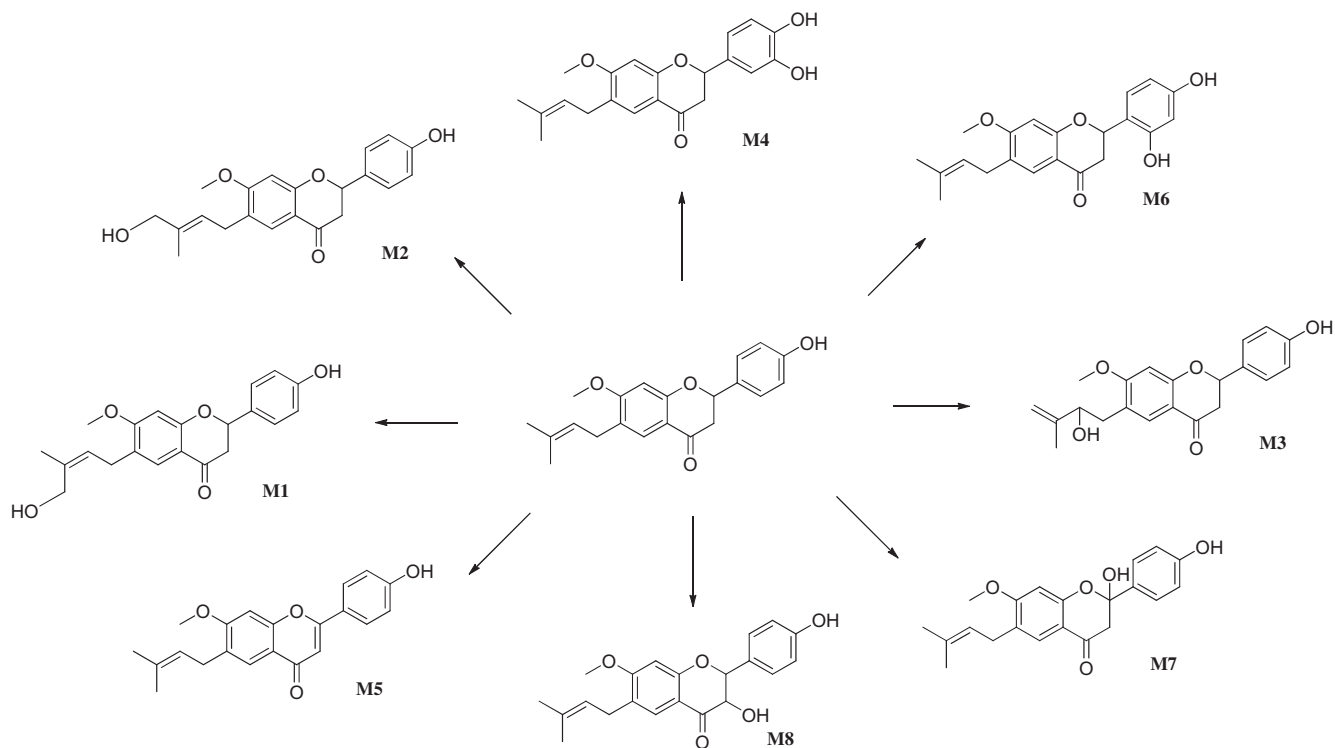
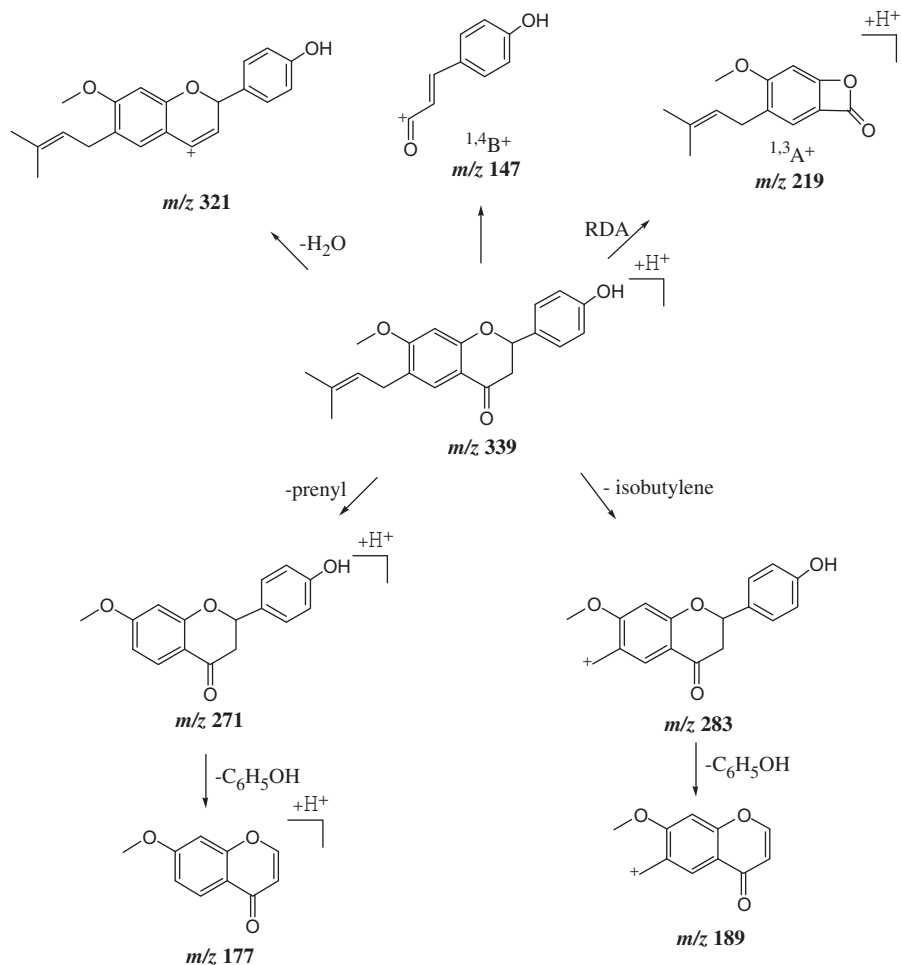


Figure 5. Proposed metabolic profile of bavachinin in rat liver microsomes.

through a loss of isobutylene chain $[(\text{CH}_3)_2\text{C}=\text{CH}_2]$ from the ion at m/z 337. In addition, the presence of fragment ion at m/z 219 from the RDA reaction, indicated that ring A was intact. To support this result, 4'-hydroxy-7-methoxy-6-(3-methyl-2-butenyl)-flavone was synthesized, and the retention time in the TIC and its molecular weight were compared with those of **M5**.

Abundant fragmentations in the product ion tandem mass spectra of **M7** and **M8** were detected at m/z 219 (Figure 3H, I), suggesting that ring A was intact. In addition, the elution times of **M7** and **M8** were different from those for **M4** and **M6**, indicating that ring C was oxidized. $^{1,3}\text{B}^+$ ion at m/z 137 and $^{0,2}\text{B}^+$ ion at m/z 121 in the MS^2 spectrum of **M8** suggested that C-3 was oxidized, whereas **M7** may be 2,4'-dihydroxy-7-methoxy-6-(3-methyl-2-butenyl)-flavanone.

Conclusions

Although prenylated flavonoids occur in various plant species, little is known about metabolism of these natural products. Therefore, this study on bavachinin metabolism develops the understanding of prenylated flavonoid metabolism. In this study, bavachinin was fragmented into eight metabolites in rat liver microsomes. The structures were proposed through a LC-ESI- MS^n analysis and chemical synthesis (Figure 5). The results indicate that the eight metabolites were biotransformed mainly through oxidation. Our investigation provides much information on the *in vitro* metabolism of bavachinin and contributes to the understanding of *in vivo* bavachinin metabolism.

Acknowledgements

The authors are grateful to Prof. Wang Chang Hong (Shanghai R&D Center for Standardization of Traditional Chinese Medicines) for the gift of liver microsomes.

Declaration of interest

The authors report no conflicts of interest.

This study was supported by a grant of Natural Science Foundation of Shanghai (13ZR1441700).

References

Aura AM, Martin-Lopez P, O'Leary KA, et al. (2005). *In vitro* metabolism of anthocyanins by human gut microflora. *Eur J Nutr* 44:133–42.

Bi YF, Zhuang XY, Zhu HB, et al. (2015). Studies on metabolites and metabolic pathways of bulleyaconitine A in rat liver microsomes using LC- MS^n combined with specific inhibitors. *Biomed Chromatogr* 29:1027–34.

Boersma MG, Woude HVD, Bogaards J, et al. (2002). Regioselectivity of phase II metabolism of luteolin and quercetin by UDP-glucuronosyl transferases. *Chem Res Toxicol* 15:662–70.

Chen J, Lin HM, Hu M. (2005). Absorption and metabolism of genistein and its five isoflavone analogs in the human intestinal Caco-2 model. *Cancer Chemother Pharmacol* 55:159–69.

Chen QH, Li Y, Chen ZL. (2012). Separation, identification, and quantification of active constituents in *Fructus psoraleae* by high-performance liquid chromatography with UV, ion trap mass spectrometry, and electrochemical detection. *J Pharmaceut Anal* 2:143–51.

Chen X, Shen YB, Liang QK, et al. (2014). Effect of bavachinin and its derivatives on T cell differentiation. *Int Immunopharmacol* 19:399–404.

Chen X, Wen T, Wei J, et al. (2013). Treatment of allergic inflammation and hyperresponsiveness by a simple compound, Bavachinin, isolated from Chinese herbs. *Cell Mol Immunol* 10:497–505.

Chen Z, Jin K, Gao LY, et al. (2010). Anti-tumor effects of bakuchiol, an analogue of resveratrol, on human lung adenocarcinoma A549 cell line. *Eur J Pharmacol* 643:170–9.

Chigurupati S, Dhanaraj SA, Balakumar P. (2015). A step ahead of PPAR γ full agonists to PPAR γ partial agonists: therapeutic perspectives in the management of diabetic insulin resistance. *Eur J Pharmacol* 755:50–7.

Chopra B, Dhingra AK, Dhar KL. (2013). *Psoralea corylifolia* L. (Buguchi)-Folklore to modern evidence: review. *Fitoterapia* 90:44–56.

Fabre N, Rustan I, Hoffmann ED, et al. (2001). Determination of flavone, flavonol, and flavanone aglycones by negative ion liquid chromatography electrospray ion trap mass spectrometry. *J Am Soc Mass Spectrom* 12:707–15.

Guo JN, Weng XC, Wu H, et al. (2005). Antioxidants from a Chinese medicinal herb – *Psoralea corylifolia* L. *Food Chem* 91:287–92.

Huang YW, Liu XY, Wu YC, et al. (2014). Meroterpenes from *Psoralea corylifolia* against *Pyricularia oryzae*. *Planta Med* 80:1298–303.

Kim DW, Seo KH, Curtis-Long MJ, et al. (2014). Phenolic phytochemical displaying SARS-CoV papain-like protease inhibition from the seeds of *Psoralea corylifolia*. *J Enzyme Inhib Med Chem* 29:59–63.

Lau KM, Wong JH, Wu YO, et al. (2014). Anti-dermatophytic activity of bakuchiol: *in vitro* mechanistic studies and *in vivo* tinea pedis-inhibiting activity in a guinea pig model. *Phytomedicine* 21:942–5.

Lee HS, Ji HY, Park EJ, et al. (2007). *In vitro* metabolism of eupalitin by multiple cytochrome P450 and UDP-glucuronosyltransferase enzymes. *Xenobiotica* 37:803–17.

Li WD, Yan CP, Wu Y, et al. (2014). Osteoblasts proliferation and differentiation stimulating activities of the main components of *Fructus Psoraleae corylifoliae*. *Phytomedicine* 21:400–5.

Luo JM, Liang QK, Shen YB, et al. (2014). Biotransformation of bavachinin by three fungal cell cultures. *J Biosci Bioeng* 117:191–6.

Ma SN, Zheng C, Feng L, et al. (2015). Microbial transformation of prenylflavonoids from *Psoralea corylifolia* by using *Cunninghamella blakesleeana* and *C. elegans*. *J Mol Catal B Enzym* 118:8–15.

Ma YL, Li QM, Heuvel VD, et al. (1997). Characterization of flavone and flavonol aglycones by collision-induced dissociation tandem mass spectrometry. *Rapid Commun Mass Spectrom* 11:1357–64.

Matsuda H, Sugimoto S, Morikawa T, et al. (2007). Bioactive constituents from Chinese natural medicines. XX. Inhibitors of antigen-induced degranulation in RBL-2H3 cells from the seeds of *Psoralea corylifolia*. *Chem Pharm Bull* 55:106–10.

Nepal M, Choi HJ, Choi BY, et al. (2012). Anti-angiogenic and anti-tumor activity of Bavachinin by targeting hypoxia-inducible factor-1 α . *Eur J Pharmacol* 691:28–37.

Nikolic D, Li Y, Chadwick LR, et al. (2005). Metabolism of xanthohumol and isoxanthohumol, prenylated flavonoids from hops (*Humulus lupulus* L.), by human liver microsomes. *J Mass Spectrom* 40:289–99.

Nikolic D, Li YM, Chadwick LR, et al. (2004). Metabolism of 8-Prenylnaringenin, a potent phytoestrogen from hops (*Humulus lupulus*), by human liver microsomes. *Drug Metab Dispos* 32:272–9.

Pharmacopoeia Committee of P.R. China. (2010). Pharmacopoeia of People's Republic of China. Beijing (China): Chin Med Sci Technol Publisher.

Quintieri L, Palatini P, Nassi A, et al. (2008). Flavonoids diosmetin and luteolin inhibit midazolam metabolism by human liver microsomes and recombinant CYP 3A4 and CYP3A5 enzymes. *Biochem Pharmacol* 75:1426–37.

Si DY, Wang Y, Zhou YH. (2009). Mechanism of CYP2C9 inhibition by flavones and flavonols. *Drug Metab Dispos* 37:629–34.

Simons R, Vincken JP, Bakx EJ, et al. (2009). A rapid screening method for prenylated flavonoids with ultra-high-performance liquid chromatography/electrospray ionisation mass spectrometry in licorice root extracts. *Rapid Commun Mass Spectrom* 23:3083–93.

Singh MP, Pathak D, Sharma GK, et al. (2011). Peroxisome proliferator-activated receptors (PPARs): a target with a broad therapeutic potential for human diseases: an overview. *Pharmacologyonline* 2:58–89.

- Su S, Wang YN, Bai L, et al. (2015). Structural elucidation of *in vivo* metabolites of isobavachalcone in rat by LC-ESI-MSⁿ and LC-NMR. *J Pharmaceut Biomed* 104:38–46.
- Sun NJ, Woo SH, Cassady JM, et al. (1998). DNA polymerase and topoisomerase II inhibitors from *Psoralea corylifolia*. *J Nat Prod* 61: 362–6.
- Wang Y, Ho CT. (2009). Metabolism of flavonoids. *Forum Nutr Basel, Karger* 61:64–74.
- Xiao GD, Li GW, Chen L, et al. (2010). Isolation of antioxidants from *Psoralea corylifolia* fruits using high-speed counter-current chromatography guided by thin layer chromatography-antioxidant autographic assay. *J Chromatogr A* 1217:5470–6.

- Xu MJ, Wu B, Ding T, et al. (2012). Simultaneous characterization of prenylated flavonoids and isoflavonoids in *Psoralea corylifolia* L. by liquid chromatography with diode-array detection and quadrupole time-of-flight mass spectrometry. *Rapid Commun Mass Spectrom* 26: 2343–58.
- Yin S, Fan CQ, Wang Y, et al. (2004). Antibacterial prenylflavone derivatives from *Psoralea corylifolia*, and their structure-activity relationship study. *Bioorgan Med Chem* 12: 4387–92.
- Zhang YZ, Xu F, Zhang JY, et al. (2014). Investigations of the fragmentation behavior of 11 isoflavones with ESI-IT-TOF-MSⁿ. *J Chin Pharm Sci* 23:631–41.